

Error accounting in electron counting experiments

Michael Wulf^{1,*} and Alexander B. Zorin¹

¹*Physikalisch Technische Bundesanstalt, Bundesallee 100, 38116 Braunschweig, Germany*

(Dated: March 12, 2022)

Electron counting experiments attempt to provide a current of a known number of electrons per unit time. We propose architectures utilizing a few readily available electron-pumps or turnstiles with the typical error rates of 1 part per 10^4 with common sensitive electrometers to achieve the desirable accuracy of 1 part in 10^8 . This is achieved not by counting all transferred electrons but by counting only the errors of individual devices; these are less frequent and therefore readily recognized and accounted for. We thereby ease the route towards quantum based standards for current and capacitance.

PACS numbers: 73.23.Hk, 06.20.-f, 85.35.Gv

In 1990 the national metrological institutes adopted the Josephson Volt [1, 2] and von Klitzing Ohm [3] as quantum based metrological units in addition to the conventional SI units. Even earlier it had been realized [4, 5] that a third electric quantum based standard would allow interesting experiments to cross-check the theories describing Josephson and quantum Hall effect. Particular interest has been spent on developing a current standard based on counting all electrons flowing in a given time interval through a constraint. While a quantum current standard is highly desirable, an experimentally more feasible alternative is an electron counting based capacitance standard (ECCS): Using N electrons to charge a capacitor to a voltage U allows to establish the devices capacitance $C = Ne/U$. U can be traced back to the Josephson quantum voltage standard, while e is the electron charge, thereby C is traced back to quantum units. As capacitance can also be calculated for certain geometries [6], this were to enable a comparison of two different ways to standardize capacitance, but even for the ECCS the engineering challenges have not yet been met in a reliable fashion, though a prototype has been demonstrated [7]. To surpass past achievement the uncertainty in the number of counted electrons has to be reduced to 10^{-8} , complicating the task at hand. While capacitance metrology requires only small currents, current metrology only becomes possible if currents in excess 1 nA can be supplied [8]. This can be achieved by using pump frequencies much higher than those that have shown satisfactory accuracy or by parallelization of devices. A higher operation frequency increases the error-rates significantly [9], while parallelization efforts are hindered by conflicting requirements on the devices, including yield and accuracy. We propose here a concept to alleviate both concerns.

The most advanced ECCS experiments use multi-stage devices referred to as electron-pumps, shown in fig. 1(a). These utilize successive quantum tunneling between metallic islands connected via tunnel-junctions. Jensen and Martinis [10, 11] recognized that electron pumps of several tunnel-junctions should be able to provide a charge with metrologically relevant precision. While relative errors of 10 ppb have been reported in a 7-junction electron pump [7], this scheme still

requires continued research to be robust enough as a metrological standard; device yield is low, operation is complicated by the number of junctions employed and the remaining error-rate is not theoretically understood. The primary error in electron pumps is believed to be caused by electron co-tunneling processes of order $N - 1$, where N is the number of junctions in the device [10]. These can be suppressed by connecting resistors in series with the pump; the resulting device is called the R-pump [12]. Other methods to achieve this goal include the use of smaller or larger number of tunnel junctions; both paths reduce yield while the latter also complicates operation. Recently approaches based on simpler devices controlled by only a single gate have received renewed attention. Quantized currents have been observed in single-gate devices made in superconducting [13] and in semiconducting technology [14, 15], as well as in superconductor-metal hybrid structures [16]. Due to their operational simplicity these approaches may be best suited for parallelization. While these technologies may be operated also at frequencies higher than those employed in the metallic electron-pump experiments, thereby increasing available current, error-rates have not been established for them and may prove to be higher than 10^{-8} . Recently three-stage R-pumps have shown reasonable operation at 100 MHz as well [9].

Architectures for discrete step error accounting - Instead of optimization of single devices, we propose to use two R-pumps (or electron-pumps) with rather high relative error rates of $2\Gamma^R = 10^{-5}$ and sufficiently long hold times. A schematic for the experiment is shown in fig. 1(b). The two R-pumps are connected in series with an intermediate node, whose charge is monitored by a sensitive electrometer, such as the RF-SET [17]. In this architecture the left pump starts by pumping \tilde{n} electrons onto the intermediate node with pump-frequency Ω_P . In addition to errors of this first pump, a charge may tunnel through the entire second pump. The rate 2λ at which this occurs is the inverse of the mean hold-time; the latter having been reported to be about 10 s for five-junction electron-pumps [11] and 16 s for the three-junction R-pump [18]. For simplicity we assume that all errors occur with equal chance for either sign; then the probability $p(n)$ for n charges to be on the node after this first pump sequence is to leading order, $p(\tilde{n} \pm 1) \simeq \tilde{n}\Gamma^R(1 - 2\lambda\frac{\tilde{n}}{\Omega_P}) + \lambda\frac{\tilde{n}}{\Omega_P}(1 - 2\tilde{n}\Gamma^R) \ll 1$, which is dominated by the first term for relevant parameters.

*Electronic address: michael.wulf@ptb.de

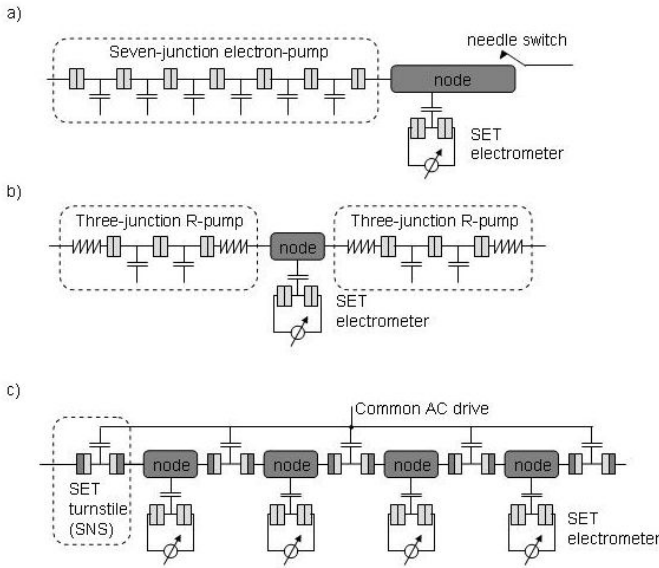


FIG. 1: (a) Circuit schematic of an electron pump with seven tunnel junctions [7]. The drives applied to the six intermediate islands are triangular pulses in carefully chosen phase-relationships. The electrometer on the final node is needed to verify device operation. A cryogenic needle switch makes contact to the chip to reversibly connect the pump to a cryo-capacitor. (b) Schematic of experiment with two sequential R-pumps and one intermediate node; resistors are drawn in red. The cryogenic switch can be removed from this device. (c) Schematic of proposed circuit of five single-gate pump devices, here based on the SNS-turnstiles of [16]. These are connected in series with the intermediate nodes monitored by four electrometers. Capacitively coupled DC leads to the intermediate islands (not shown) allow adjustment of the required voltage-offsets of the SNS pumps, while all pump-gates are subjected to the same sinusoidal AC bias.

After the first pump phase the electrometer is used to measure the number of electrons on the node. RF-SETs [17] are among the suitable electrometers for this purpose. Several laboratories have built RF-SETs with charge resolution of about $\sigma_q = 10^{-5}e/\sqrt{\text{Hz}}$ [17, 19] and even a ten-fold improvement over these numbers has been demonstrated [20]. Typical bandwidths exceed 10 MHz, which is sufficient for the needs of this work. An alternative readout is provided by inductively shunted SETs [21, 22, 23], which may achieve similar charge resolution. A coupling capacitance of $C_C = 100$ aF between the electrometer's gate and the intermediate node is consistent with maintaining this charge-resolution. If the nodes self-capacitance is $C_{\text{node}} = 2.5$ fF, the effective charge-resolution is only reduced by a factor of $C_{\text{node}}/C_C = 25$. With the parameters stated, the probability of a measurement error using $10\mu\text{s}$ of integration time is less than 10^{-9} . C_{node} is nonetheless large enough for stable operation of the pumps as each electron will produce a voltage of only about 60 nV on this node. \tilde{n} has to be kept below ~ 1000 , as the three-junction R-pump has a stable operation window of $100\mu\text{V}$, with respect to the voltage across it [18]. The measurement is followed by a pump-sequence of the second pump, emptying the node into the second reservoir. Subsequently a sec-

ond measurement establishes the nodes charge state at the end of the cycle, which thereafter can be repeated. If during either measurement the charge on the island is found to deviate from the value expected due to the design of pump-cycles, this deviation is attributed to errors of the pump that was active since the previous measurement. This assumption will be correct unless either, the second pump experienced a hold error, or if one of the two measurements was wrong. The probabilities for each sign being $p_{\text{hold}}^{\text{error}} < (\tilde{n}/\Omega_P + 2\tau_m)\lambda$ and $p_{\text{measure}}^{\text{error}} = (1 - \text{erf}(\frac{eC_C\sqrt{\tau_m}}{C_{\text{node}}\sigma_q} - .5))/2$. Errors produced by the active pump are properly recognized and can thus be accounted for, therefore the unaccounted errors no longer scale with Γ^R . Depending on the architecture, it may suffice to identify the errors made. Alternatively, feedback mechanisms could be provided after error-detection, for example by altering the number of pump-cycles, to counter a detected error. Such feedback mechanisms will be more device specific than the scope of the present work and are therefore left out here. Three-junction R-pumps have been operated at frequencies as high as $\Omega_P = 100$ MHz [9]. With the parameters as stated and $\tilde{n} = 1000$ the corrected relative error-rate becomes $\Gamma_{\text{corr}}^R = 2(p_{\text{hold}}^{\text{error}} + p_{\text{measure}}^{\text{error}})/\tilde{n} = 9 \cdot 10^{-9}$; accordingly this proposed circuit reaches the metrologically necessary accuracy. A further improvement may be achieved by use of a third pump and a second intermediate island. The above method allows recognition of the number of errors per cycle, which are then attributed to the active device. With the additional island the signatures of the errors for each of the three pumps differ: If an error occurs on the left or right pump, only the charge on the corresponding island deviates from expectation, while the charges on both islands do in opposite directions whenever an error occurs on the middle pump. As both nodes are monitored these errors can therefore be distinguished and accounted for, though measurement errors remain. Furthermore, errors involving two R-pumps may be indistinguishable from errors of the remaining one. The probability of any of these errors occurring during a complete cycle comprised of three pump- and measurement-phases is approximated to the first order by $p_3 = 6(\tilde{n}/\Omega_P + 2\tau_m)\lambda(2\tau_m\lambda + \tilde{n}\Gamma^R) + 6p_{\text{measure}}^{\text{error}}$, and the corrected relative error rate becomes $2\Gamma_{\text{corr},3}^R = p_3/\tilde{n}$. Even devices with performance values of $2\Gamma_R = 10^{-4}$, $\lambda = 1$ Hz, $\Omega_P = 100$ MHz suffice to provide the metrological requirement, achieving $2\Gamma_{\text{corr},3}^R = 6 \cdot 10^{-9}$ for $\tilde{n} = 53$ with an effective pump-rate reduced to 16.6 MHz. The operation even of three low-quality R-pumps in series is expected to be experimentally less challenging than the operation of a single near perfect device; the same is likely regarding fabrication yield. In addition, the proposed architecture allows the error-rates to be continuously monitored during operation, and thereby in-situ minimization of error rates through dynamic adjustment of external biases. This is not possible in the conventional ECCS experiments [24], as single electrons can no longer be detected on the pumps final node once is connected to the external capacitor. In the conventional ECCS experiment the electron-pump operation is only optimized while the final node is isolated from the external capacitor; then the electrometer allows detection of single electrons on this node, allowing optimization by shuttling a few electrons back and

forth through the pump. Afterwards the pump is connected to the capacitor by means of a needle switch contacting onto this node. Misaligned needle-switches may damage devices; furthermore the mechanical force inherent in the switching process may shift the charge offsets on the islands due to the piezo-electric effect [25]. In contrast, the proposed architecture allows the switches removal from the chip containing the pump-devices, and thereby further simplification of the experiment.

Architectures for continuous error accounting - The circuit with two nodes and three pumping devices, allows further improvement. Even a modest relative error-rate of 10 ppm and an operation frequency of 100 MHz yields on average only 1000 errors per pump per second. Such rare errors are readily resolved, even while all three pumps operate continuously. Without pump-errors the charge on the nodes were to remain constant, or only be modulated at the pump frequency, while perfect and instant measurements of the node charges allow for all pump-errors to be detected and properly attributed according to the rules stated above. But due to the finite charge-resolution of available electrometers, there is a time τ_M , during which errors occurring, nearly simultaneously, in two of the pumps may be indistinguishable from an error of the third device. The chance for each of these six relevant second order scenarios to occur within one measurement time is just $P_E = (\Omega_P \Gamma^R \tau_M)^2$. With $\Omega_P = 1$ MHz, $\Gamma^R = 10^{-5}$ and $\tau_M = 15$ μ s we recover $P_E = 2.25 \cdot 10^{-8}$. If the information from the measurements is then used to identify the single-pump-errors and correct or account for them, the reduced, relative error rate becomes of order $2\gamma_3^R = 6P_E/\tau_M\Omega_P = 6(\Omega_P\Gamma^R\tau_M)\Gamma^R$ which computes to $2\gamma_3^R = 9 \cdot 10^{-9}$, beating current metrological requirements. When not three but $2N + 1$ pumps are used, the dominating error, that is not properly recognized, is of order $N + 1$ so that the leading term in the relative error rate scales as

$$2\gamma_{2N+1}^R = 2 \frac{(2N+1)!}{N!(N+1)!} (\Omega_P \Gamma^R \tau_M)^N \Gamma^R. \quad (1)$$

Note that the error rate decreases exponentially with the number of devices included. As both pump operation and measurements are continuous, the following more complete approach is needed.

For a circuit of $2N + 1$ pumps with independent errors with rates $2\alpha = 2\Gamma^R\Omega_P$ with respect to time the joint probabilities of n_i errors having occurred at pump i obey, with $\vec{n} = \{n_1, n_2, \dots, n_{2N+1}\}$, the n-dimensional diffusion-equation

$$\dot{P}_{\vec{n}}(t) = -2N\alpha P_{\vec{n}}(t) + \sum_{|\vec{n}-\vec{m}|=1} \alpha P_{\vec{m}}(t). \quad (2)$$

The $(2N + 1)$ -dimensional set of probabilities, $P_{\vec{n}}$, can be rearranged as a vector, \vec{P} . This allows rewriting of eq. (2) as $\dot{\vec{P}}(t) = T\vec{P}(t)$, defining operator T . This diffusion corresponds to the errors in conventional electron pumping experiments, while in our circuit this diffusion is observed by the electrometers. The perceived probabilities of the number of errors that have occurred will depend on the diffusion of eq. (2) as well as the result of the measurement outcomes of the

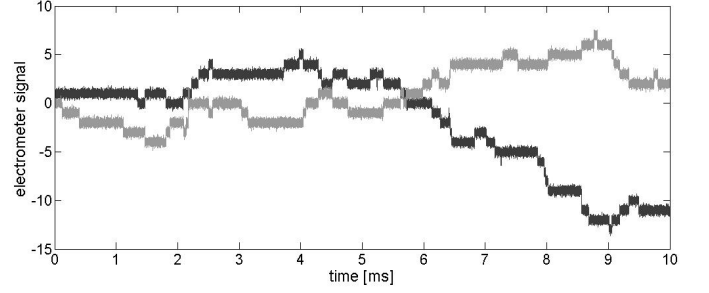


FIG. 2: Signal traces of first (black) and second (gray) electrometer. Black and red lines indicate ideal measurement results without noise. Pump-error rates are 1000/s, per pump and sign, electrometer noise $10^{-5}e/\sqrt{\text{Hz}}$, coupling capacitance ratio $C_C/C_{\text{node}} = 0.04$, signal averaged over 200 ns.

$N - 1$ intermediate electrometers, $\{x_1(t), \dots, x_{N-1}(t)\}$. In the absence of diffusion and due to the measurements alone $\Pi_{\vec{n}}$, the perceived probabilities of \vec{n} errors having occurred divided by the probability of $\vec{n}_0 = \{0, 0, \dots\}$ errors having occurred, develop according to

$$\dot{\Pi}_{\vec{n}} = \left[\sum_{i=1}^{N-1} (2(n_i - n_{i+1})x_i - (n_i - n_{i+1})^2)/\beta_i \right] \Pi_{\vec{n}}. \quad (3)$$

Here β_i denotes the rms-mean of the noise of the electrometer i , normalized by the single-electron signal, which is assumed to be gaussian and white. This equation can be rewritten to yield $\vec{\Pi}(t) = U(t)\vec{\Pi}(t)$. Observe that U is stochastic and includes information about the instantaneous electrometer signal, which in turn is a function of the instantaneous electrometer noise as well as the diffusion history.

In the scenario of interest both processes coexist; from the measured traces of the electrometer signals we extract the evolution of the perceived relative probabilities, $\vec{\pi}$, as

$$\dot{\vec{\pi}} = (T + U)\vec{\pi}. \quad (4)$$

Figure (2) shows a typical set of signal traces that can be expected from the combination of the diffusion dynamics and likely electrometer noise. These traces are used to numerically integrate eq. (4) yielding a perceived diffusion. Figure 3 contains a histogram of the result of 12500 generated diffusions contrasted with the effective error resulting when for each trace the perceived diffusion is subtracted from the underlying diffusion, yielding the error despite correction. The latter corresponds as well to a diffusion, albeit with a reduced diffusion (or error) rate. Numerical results for these reduced error rates are shown for various parameters in fig. 4 in excellent agreement with eq. (1). Note that even for a rate of 200 errors per second a 10000-fold improvement of the error rate is achieved with only three pumps and two intermediate electrometers, so that even devices exhibiting a relative error-rate of 100 ppm can reach the metrologically desirable error threshold of 10 ppb due to the proposed architecture. The five pump version achieves a similar improvement even at a rate of 8000 errors per second. For devices with a relative error-rate

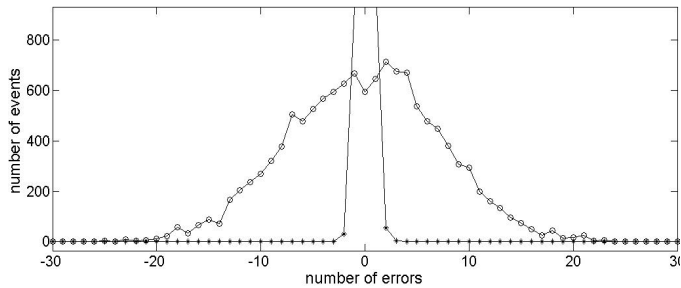


FIG. 3: Histogram of the errors (circles) and errors after correction (stars) of 12500 traces of 30 ms with an error rate of 1000/s, other parameters as in fig. (2). The peak corresponding to proper recognition of all errors is suppressed for clarity.

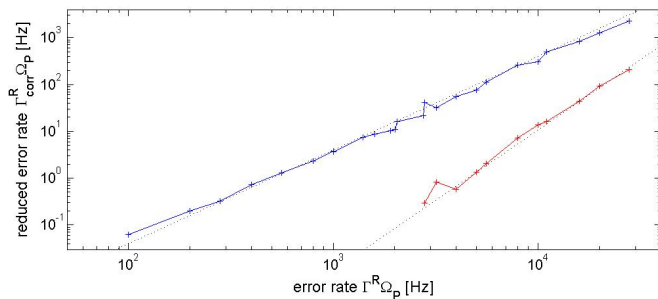


FIG. 4: Corrected error rates with respect to time for three (upper curve) and five (lower curve) pump circuits as a function of the uncorrected error rates. Dashed lines are a fit to eq. (1). Other parameters as in fig. 2.

of 100 ppm, this would allow pump rates of 2 MHz for three

devices or 80 MHz for five. If however devices with a relative error-rate of 10 ppm were available, only a thousandfold improvement were required; this could be achieved with a five-pump architecture and a pump frequency of approximately 1 GHz. The latter example not only achieves the required accuracy for a metrological current standard, but achieves this with sufficiently large current for applications such as cross-checking the relations of the metrological triangle of electrical units.

In summary, we have proposed a family of architectures utilizing either conventional electron pumps of modest quality or one of the single-gate devices that are capable of producing quantized current steps with the now common RF-SET or a similar device. The algorithm employed in this work determines the charge transported by such structure to a much greater precision than would be feasible by any single of the devices used. The relaxation on the requirements for the quality of the individual devices used, simplifies experimentation, even at higher operation frequency, and increases sample yield. It thereby opens the prospects towards parallelization needed to increase the provided current. We note that the proposed architecture allows to monitor the error-rates of individual pumps on the level of single electrons, similar to those stated for electron-pumps in their shuttle mode. This has not been possible for the single gate devices [13, 15, 16] in currently employed circuits. Accordingly the architecture proposed here allows further research on these devices and thereby a determination regarding their suitability for metrological applications, while easing the required thresholds.

This work is supported in part by the European Union under the Joint Research Project REUNIAM as well as through the project EuroSQIP. M. W. gratefully acknowledges discussions with M. J. Feldman on the early stages of this work.

-
- [1] M. T. Levinson, R. Y. Chia, M. J. Feldman and B. A. Tucker, *Appl. Phys. Lett.* **31**, 776 (1977).
- [2] J. Kohlmann, R. Behr and T. Funck, *Meas. Sci. Technol.* **14**, 1216 (2003).
- [3] K. von Klitzing, *Phil. Trans. R. Soc. A* **363**, 2203 (2005).
- [4] K. K. Likharev and A. B. Zorin *Jour. Low Temp. Phys.* **59**, 347 (1985).
- [5] J. Gallop, *Phil. Trans. R. Soc. A* **363**, 2221 (2005).
- [6] W. K. Clothier, *Metrologia* **1**, 36 (1965).
- [7] M. W. Keller, A. L. Eichenberger, J. M. Martinis, N. M. Zimmerman, *Science* **285**, 1706 (1999).
- [8] M. W. Keller, in *proceedings of Fermi school CXLVI: Recent Advances in Metrology and Fundamental Constants* (2001).
- [9] B. Steck, A. Gonzalez-Cano, N. Feltn, L. Devoille, F. Piquemal, S. Lotkhov and, A. B. Zorin *Metrologia* **45**, 482 (2008).
- [10] H. D. Jensen and J. M. Martinis, *Phys. Rev. B* **46**, 13407 (1992).
- [11] J. M. Martinis, M. Nahum and H. D. Jensen, *Phys. Rev. Lett.* **72**, 904 (1994).
- [12] S. V. Lotkhov, S. A. Bogoslovsky, A. B. Zorin and J. Niemeyer, *Appl. Phys. Lett.* **78**, 946 (2001).
- [13] L. J. Geerligs et al. *Phys. Rev. Lett.* **64**, 2691 (1990).
- [14] B. Kaestner, V. Kashcheyevs, G. Hein, K. Pierz, U. Siegner, and H. W. Schumacher, *Appl. Phys. Lett.* **92**, 192106 (2008).
- [15] M. D. Blumethal, B. Kaestner, L. Li, S. Giblin, T. J. B. M. Janssen, M. Pepper, D. Anderson, G. Jones, and D. A. Ritchie, *Nature Physics* **3**, 343 (2007).
- [16] J. P. Pekola, J. J. Vartiainen, M. Mtnen, O.-P. Saira, M. Meschke, and D. V. Averin, *Nature Physics* **4**, 120 (2007).
- [17] R. J. Schoelkopf, P. Wahlgren, A. A. Kozhevnikov, P. Delsing, D. E. Prober, *Science* **280**, 1238 (1998).
- [18] H. Scherer, S. V. Lotkhov, G.-D. Willenberg, and A. B. Zorin, *IEEE Trans. on Instr. and Meas.* **54**, 666 (2005).
- [19] J. Bylander, T. Duty and P. Delsing, *Nature* **434**, 361 (2005).
- [20] H. Brenning, S. Kafanov, T. Duty, S. Kubatkin and P. Delsing, *Jour. Appl. Phys.* **100**, 114321 (2006).
- [21] A. B. Zorin, *Phys. Rev. Lett.* **86**, 3388 (2001).
- [22] M. A. Sillanpää, L. Roschier, P. J. Hakonen, *Phys. Rev. Lett.* **93**, 066805 (2004).
- [23] A. B. Zorin *Physica C* **368**, 284 (2002).
- [24] M. W. Keller, J. M. Martinis, A. H. Steinbach, and N. M. Zimmerman, *IEEE Tran. Instr. and Meas.* **46**, 307 (1997).
- [25] M. W. Keller, private communications.